

Nanomeasurements of electronic and mechanical properties of fullerene embedded Si(111) surfaces

Chih-Pong Huang, Chih-Chuan Su, Wan-Sheng Su, Chiao-Fang Hsu, and Mon-Shu Ho

Citation: *Appl. Phys. Lett.* **97**, 061908 (2010); doi: 10.1063/1.3475775

View online: <http://dx.doi.org/10.1063/1.3475775>

View Table of Contents: <http://apl.aip.org/resource/1/APPLAB/v97/i6>

Published by the [American Institute of Physics](#).

Related Articles

Morphology and porosity of nanoporous Au thin films formed by dealloying of AuSi_{1-x}
J. Appl. Phys. **112**, 094320 (2012)

Diamondoid coating enables disruptive approach for chemical and magnetic imaging with 10nm spatial resolution
Appl. Phys. Lett. **101**, 163101 (2012)

Modified Faraday rotation in a three-dimensional magnetophotonic opal crystal consisting of maghemite/silica composite spheres
Appl. Phys. Lett. **101**, 151121 (2012)

Assembled Fe_3O_4 nanoparticles on graphene for enhanced electromagnetic wave losses
Appl. Phys. Lett. **101**, 153108 (2012)

Highly versatile ultra-low density GaAs quantum dots fabricated by filling of self-assembled nanoholes
Appl. Phys. Lett. **101**, 143106 (2012)

Additional information on *Appl. Phys. Lett.*

Journal Homepage: <http://apl.aip.org/>

Journal Information: http://apl.aip.org/about/about_the_journal

Top downloads: http://apl.aip.org/features/most_downloaded

Information for Authors: <http://apl.aip.org/authors>

ADVERTISEMENT



Goodfellow
metals • ceramics • polymers • composites
70,000 products
450 different materials
small quantities fast

www.goodfellowusa.com

Nanomeasurements of electronic and mechanical properties of fullerene embedded Si(111) surfaces

Chih-Pong Huang,¹ Chih-Chuan Su,¹ Wan-Sheng Su,² Chiao-Fang Hsu,¹ and Mon-Shu Ho^{1,3,a)}

¹Department of Physics, National Chung Hsing University, Taichung 402, Taiwan

²Department of Physics, National Cheng Kung University, Tainan 700, Taiwan and Center for General Education, Tainan University of Technology, Tainan 710, Taiwan

³Institutes of Nanoscience and Biophysics, National Chung Hsing University, Taichung 402, Taiwan

(Received 30 April 2010; accepted 16 July 2010; published online 11 August 2010)

This study describes the feasibility of fabricating of a single layer of fullerene embedded Si surface through a controlled self-assembly mechanism in an ultrahigh vacuum (UHV) chamber. The characteristics of the fullerene embedded Si surface are investigated directly using UHV-scanning probe microscopy. Additionally, the band gap energy and field emission parameters, including turn-on field and the field enhancement factor β of the fullerene embedded Si substrate, are determined using a high-voltage source measurement unit and UHV-scanning tunneling microscopy, respectively. Moreover, the nanomechanical properties, which represent the stress of the fullerene embedded Si substrates, are assessed by an environment atomic force microscope (AFM) and UHV-AFM, respectively. Results of this study demonstrate that a single layer of the fullerene embedded surface has superior properties for nanotechnology applications owing to the ability to control the self-assembly mechanism of fabrication. © 2010 American Institute of Physics. [doi:10.1063/1.3475775]

The pioneering study of Feynman on nanotechnology (1959), ushered in the fabrication of several nanomaterials by controlling the material structure with assembly mechanisms.¹ Elucidating the effect of size variation in nanoscale has also led to various and unique physical and chemical properties in materials. While extending Feynman's theories to observe and manipulate atoms, Binnig and Rohrer (1981) also conducted nanomeasurements possible with scanning probe microscopy (SPM).^{1,2} Following the above developments, nanotechnology has been extensively adopted in modern science and a diverse array of applications.

Fullerene molecules and their composite materials are considered a distinctive nanomaterial owing to their excellent structural characteristics, electronic conductivity, mechanical strength, and chemical properties.^{3–6} Their applications have brought opportunities in various fields, such as electronics, computers, fuel cell technology, solar cells, and field emission technology.^{7,8} Among a wide range of potential materials, silicon/carbon (nanoparticles) composite has received considerable attention recently in device technologies because the characteristics of silicon carbide include a wide band gap, high thermal conductivity and stability, great breakdown in electronic field strength, and chemical inertness. However, conventional silicon carbides have several limitations.⁹ For instance, high density defects, including micropipes and dislocations, frequently appear on their surfaces. Such defects can even propagate into substrate materials and cause device failure.¹⁰ Although SiC preparation has been studied since 1960, this unresolved problem degrades the performance of SiC devices.^{11,12}

This study fabricates a monolayer of fullerene molecules on the Si(111) disorder surface in an UHV chamber through a controlled self-assembly process. The electronic and mechanical properties of the fullerene embedded substrate are also investigated using different surface analyses. Excellent characteristics of the developed material demonstrate of the role of nanotechnology by controlling matter on an atomic and nanoparticle scale. Results of this study indicate that the fullerene embedded silicon substrate is a highly promising alternative for semiconductor carbide in optoelectronic devices and high-temperature, high-power, or high-frequency electronic devices.^{13,14}

All experiments were performed in an ultrahigh vacuum (UHV) chamber with a variable temperature SPM.¹⁵ Fullerene deposition is achieved via a K-cell under a pressure less than 5×10^{-8} Pa at 650 °C with the preannealed silicon substrate at 800 °C for 30 min. Next, the stiffness of the fullerene embedded Si substrate in air and the UHV environment, respectively, was investigated by using an atomic force microscope (AFM). Used to evaluate the surface mechanical properties, the Si probes have a tip radius of ~ 5 – 20 nm and spring constant of ~ 40 N/m. The sample bias and the tunneling current used for UHV-scanning tunneling microscopy (STM) imaging are generally -2 V and 0.1 nA, respectively. C_{84} molecules were chosen for presentation in this paper. The field emission system was operated in a vacuum chamber at a pressure of approximately 5×10^{-5} Pa. The fullerene embedded silicon substrate functioned as the cathode, and a copper probe with a cross section area of ~ 0.71 mm² acted as the anode. The distance (d) between the cathode and anode was around 590 μ m. Additionally, the emission current was determined with a Keithley 237 high-voltage source measurement unit with a current amplifier by applying a voltage ranging from 100 to 1100 V in the field emission regime. Finally, the optoelectrical

^{a)} Author to whom correspondence should be addressed. Electronic mail: msho@dragon.nchu.edu.tw. Tel.: +886-4-22840427 Extn.: 519. FAX: +886-4-22862534.

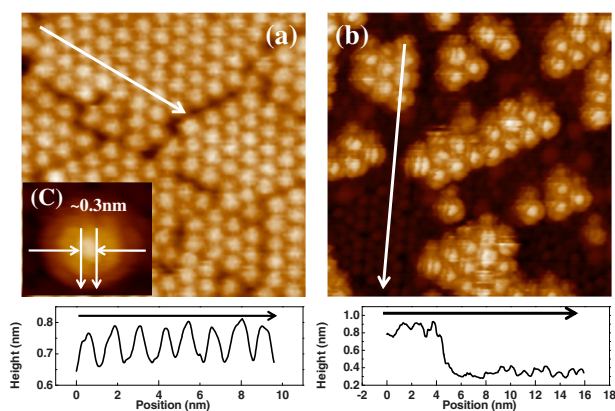


FIG. 1. (Color online) STM images with profiles analysis of (a) single C_{84} embedded Si(111) surface, (b) Si(111) superlattice surface, and (c) close up view of a C_{84} molecule on a self-assembled surface.

properties were determined based on photoluminescence (PL) emission measurement.

Annealing treatment was performed to remove surplus fullerene and form the hexagonal close-packed structure of C_{84} arrays on the surface.¹⁶ With this repeated annealing process, fullerene C_{84} molecules were considered evenly distributed on the silicon surface through a layer-by-layer growth mechanism. Figure 1(a) shows a flat and self-assembled single layer of C_{84} molecules on the Si(111)-disordered surface. The inset presents a close view of the C_{84} molecule, indicating that C_{84} molecules are aligned vertically to the Si(111) surface.¹⁷ Profile analysis of C_{84} molecules on Si(111) surface in Figs. 1(a) and 1(b) reveals that the heights and spacing are approximately 6.5 and 11.7 Å for a single C_{84} layer on an Si(111) surface. The vertical sizes of the C_{84} on Si surface are significantly smaller than its real size in free space ($9\text{Å} \times 7\text{Å}$). This indicates that the C_{84} molecules are embedded in the silicon surfaces. The C_{84} is oval-shaped with a larger height-diameter ratio approximately 1.3 compared to the ball-shaped C_{60} in free space. This increased ratio offers an improvement field emission characteristics,¹⁸ and the diameter of the top of a C_{84} molecule is only 0.3 nm on Si surface [Fig. 1(c)]. The spacing-height ratio of the C_{84} embedded Si(111) substrate is approximately ~ 1.8 , which is close to the best value (~ 2) for field emission spacing-height in simulations of patterned CNT films.¹⁹

Figure 2 shows the derivative (dI/dV) versus the voltage

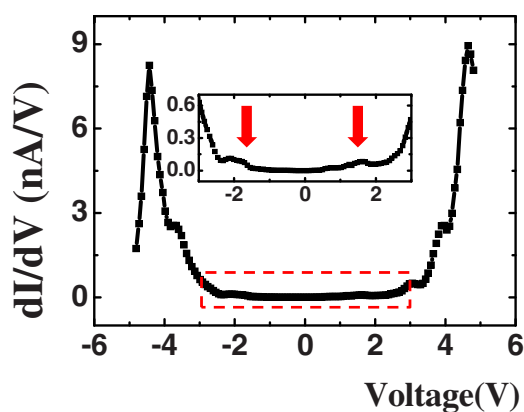


FIG. 2. (Color online) The (dI/dV) vs voltage curve of the self-assembled C_{84} embedded Si surfaces determined by UHV-STM with an enlarged scale of the z-axis in the inset.

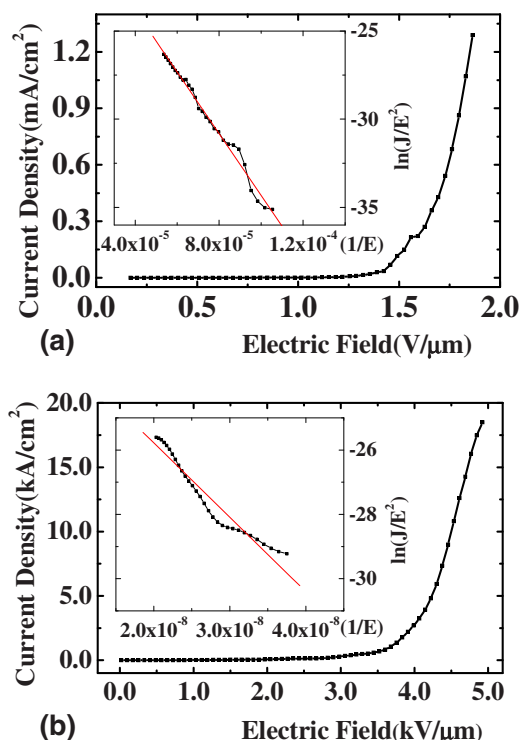


FIG. 3. (Color online) Field emission current density vs electric field curve of the self-assembled C_{84} embedded surface measured by (a) Keithley 237 source-measure unit and (b) UHV-STM, respectively. Insets show the corresponding F-N plot.

curve which corresponds to the local density of states on a substrate surface. An inset presents the (dI/dV)- V curve with an enlarged scale of the z-axis of Fig. 2. The curve reveals that the C_{84} embedded Si substrate has semiconductor properties. As is estimated, the band gap energy of C_{84} embedded Si substrate is around 3.4 ± 0.5 eV. In comparison with silicon, GaAs, and SiC, a C_{84} embedded Si substrate has a wider band gap for optoelectronic applications.²⁰ According to published data from UHV-SPM experiments,^{21,22} Si surfaces interact very energetically with hydrogen, oxygen, or nitrogen atoms at temperature above room temperature. However, a C_{84} embedded Si substrate is an inert chemical and can be removed from the UHV chamber for other studies and measurements when the C_{84} self-assembled layer is compactly arranged on the silicon surface.

Many parameters that affect field emission characteristics have been extensively studied for years to address field emission issues.^{23–25} These parameters include geometry, structure, aspect ratio, and screening effect of nanostructures. As is widely assumed, the high aspect ratio with a nanowire design array is a superior design for field emission.¹⁸ This study describes the feasibility of fabricating a self-assembled array of C_{84} layer in an UHV chamber. The C_{84} embedded Si substrate is removed from the chamber for field emission testing. Figure 3(a) shows the field emission current density versus the electric field curve of the self-assembled C_{84} layer, as measured by a Keithley 237 source-measure at room temperature. The turn-on electric field (E_{on}) is approximately $1.12\text{ V}/\mu\text{m}$ when the corresponding turn-on current density (J_{on}) reaches $1\text{ }\mu\text{A}/\text{cm}^2$. The field emission efficiency can also be evaluated by estimating the geometric enhancement factor β . According to the plot in the inset of Fig. 3(a), the field emission properties follow the corresponding Fowler–

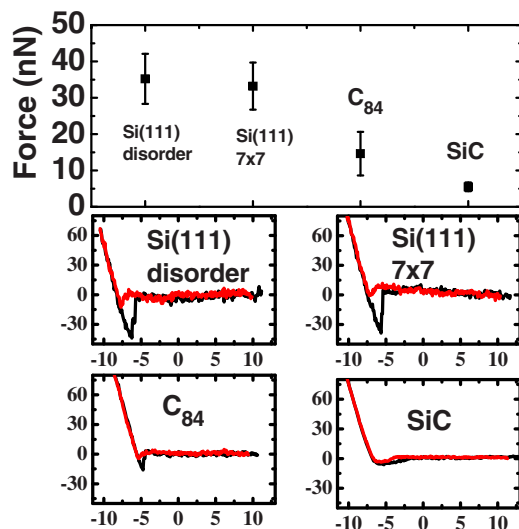


FIG. 4. (Color online) Force-distance analysis of the Si disordered surface, 7×7 surface, a single layer of the self-assembled C_{84} embedded Si surface and SiC surface by UHV-AFM.

Nordheim (FN) behavior. The field enhancement factor β can be derived from the slope of the F-N plot. Experimental results indicate that the value for the work function of fullerene molecules is around 5 eV, i.e., the same as for graphite.²⁶ According to the slope of the F-N plot, the β value is around 4.3×10^3 . In contrast with other field emission electron sources, factor β of carbon nanotubes is around 100–10 000; the value of SiC nanowires is around 10^2 – 10^3 , and $\sim 10^4$ for special designs.^{23–25} Notably, the geometric factor β of the single self-assembly layer of the fullerene embedded Si substrate in this study is rather large, while the turn on field is relatively small.

This study also reexamines the field emission properties in a UHV system through STM I-V measurements. Figure 3(b) and the inset display the J-E and F-N plots of the self-assembled C_{84} layer measured by UHV-STM at room temperature. The distance between the tip and the fullerene embedded silicon substrate is around 1 nm. The corresponding turn-on electric field (E_{on}) is approximately $1363 \text{ V}/\mu\text{m}$, while the current density (J_{on}) reaches $10^8 \mu\text{A}/\text{cm}^2$. As is estimated, the field enhancement factor β is estimated at around 3.3 in the UHV-STM system. The finding is attributed to that the geometry and diameter of the STM tip (anode) are similar to those of C_{84} molecules (cathode). They resemble parallel plates at an extremely close distance. The turn-on voltage is estimated approximately 2.2 V in a UHV system. In comparison with turn-on voltages in other studies which are around 500–3000 V,^{24,25} the result is considerably small. Moreover, the breakdown voltage of the C_{84} embedded Si substrate is obtained as $3.0 \times 10^7 \text{ V}/\text{cm}$. The optoelectronic properties are determined by PL emission measurement with a He–Cd laser source at 325 nm. The spectra revealed that the C_{84} embedded Si substrate with 3.4, 2.98, and 2.67 eV for UV and near UV light emission is highly applicable in the optoelectronic industry. The peaks of the PL data are related to electronic transition energy between conductive and valence bands. The PL data reconfirm the results of the band gap from the (dI/dV)-V measurements.

This study also determines the stiffness, adhesion and viscoelasticity of the substrate surface, referred to as material hardness based on use of the AFM. On this scale, a diamond

has a hardness of 10 (hardest); SiC has a hardness of 9; and Si has a hardness of 6–7. The nanomechanical properties of a C_{84} embedded Si substrate are characterized from the AFM force curves. Figures 4 show the force-distance curves obtained by UHV-AFM. According to these figures, the adhesion is approximately 35.2 ± 6.9 , 33.2 ± 6.5 , 14.6 ± 6.0 , and $5.5 \pm 1.2 \text{ nN}$ for clean disordered, 7×7 , C_{84} embedded Si(111) surfaces and SiC in UHV-AFM system, and 100.2 ± 13.2 , 59.0 ± 6.5 , and $32.3 \pm 4.3 \text{ nN}$ for Si(111), C_{84} embedded Si(111), and SiC surfaces in atmosphere. A lower adhesion force implies a harder material. Above results demonstrate that the hardness of the proposed C_{84} embedded Si substrate is comparable to that of SiC surfaces.

In summary, the nanocharacteristics of the C_{84} embedded Si surface are examined using various surface analysis approaches in both the atmosphere and UHV system. Experimental results indicate that the C_{84} embedded Si surface has a highly uniform distribution, a high emission efficiency and a low turn-on voltage, making it highly promising as a field emitter source. The fullerene embedded silicon surface, based on a controlled nanotechnology self-assembly mechanism, is a significant improvement in the application field of FED, optoelectronic device fabrication, and semiconductor carbide replacement.

¹R. P. Feynman, *Eng. Sci.* **23**, 22 (1960).

²G. Binnig, H. Rohrer, Ch. Gerber, and E. Weibel, *Phys. Rev. Lett.* **49**, 57 (1982).

³H. W. Kroto, J. R. Heath, S. C. O'Brien, R. F. Curl, and R. E. Smalley, *Nature (London)* **318**, 162 (1985).

⁴Z. P. Zhu and Y. D. Gu, *Carbon* **34**, 173 (1996).

⁵S. Margadonna, C. M. Brown, T. J. S. Dennis, A. Lappas, P. Pattison, K. Prassides, and H. Shinohara, *Chem. Mater.* **10**, 1742 (1998).

⁶F. Diederich, R. Ettl, Y. Rubin, R. L. Whetten, R. Beck, M. Alvarez, S. Anz, D. Sensharma, F. Wudl, K. C. Khemani, and A. Koch, *Science* **252**, 548 (1991).

⁷Z. Lv, Z. Deng, D. Xu, X. Li, and Y. Jia, *Displays* **30**, 23 (2009).

⁸K. Tokunaga, *Chem. Phys. Lett.* **476**, 253 (2009).

⁹D. K. Basa and F. W. Smith, *Thin Solid Films* **192**, 121 (1990).

¹⁰P. G. Neudeck and J. A. Powell, *IEEE Electron Device Lett.* **15**, 63 (1994).

¹¹Y. M. Tairov and V. F. Tsvetkov, *J. Cryst. Growth* **43**, 209 (1978).

¹²D. Nakamura, M. Gunjishima, S. Yamaguchi, T. Ito, A. Okamoto, H. Kondo, S. Onda, and K. Takatori, *Nature (London)* **430**, 1009 (2004).

¹³V. E. Chelnokov and A. L. Syrkin, *Mater. Sci. Eng., B* **46**, 248 (1997).

¹⁴H. Morkoç, S. Strite, G. B. Gao, M. E. Lin, B. Sverdlov, and M. Burns, *J. Appl. Phys.* **76**, 1363 (1994).

¹⁵M.-S. Ho, I.-S. Hwang, and T. T. Tsong, *Surf. Sci.* **564**, 93 (2004).

¹⁶After deposition, an annealing cycle is applied to generate a self-assembled surface. We rapidly raise the substrate temperature to 800 °C for seconds, then quench the substrate to 600 °C many times.

¹⁷C. P. Huang, C. C. Su, and M. S. Ho, *Appl. Surf. Sci.* **254**, 7712 (2008).

¹⁸W. Z. Wang, B. Q. Zeng, J. Yang, B. Poudel, J. Y. Huang, M. J. Naughton, and Z. F. Ren, *Adv. Mater.* **18**, 3275 (2006).

¹⁹L. Nilsson, O. Groening, C. Emmenegger, O. Kuettel, E. Schaller, L. Schlapbach, H. Kind, J. M. Bonard, and K. Kern, *Appl. Phys. Lett.* **76**, 2071 (2000).

²⁰The band gap energy is 1.1 eV for silicon, 1.42 eV for GaAs, 3.2 eV for 4H-SiC, 3.0 eV for 6H-SiC, and 2.3 eV for 3C-SiC.

²¹R.-L. Lo, I.-S. Hwang, M.-S. Ho, and Tien. T. Tsong, *Phys. Rev. Lett.* **80**, 5584 (1998).

²²I. K. Cho, Y. K. Kim, and H. W. Yeom, *Phys. Rev. B* **73**, 115328 (2006).

²³H. Zhang, P. X. Feng, P. Jin, V. I. Makarov, L. Fonseca, G. Morell, and B. R. Weiner, *Appl. Phys. Lett.* **95**, 061906 (2009).

²⁴J. M. Bonard, N. Weiss, H. Kind, T. Stockli, L. Forro, K. Kern, and A. Chatelain, *Adv. Mater.* **13**, 184 (2001).

²⁵Z. S. Wu, S. Z. Deng, N. S. Xu, J. Chen, J. Zhou, and J. Chen, *Appl. Phys. Lett.* **80**, 3829 (2002).

²⁶A. V. Karabutov, V. D. Frolov, and V. I. Konov, *Diamond Relat. Mater.* **10**, 840 (2001).